Optimal Control of Unmanned Aerial Vehicles Electric Launcher

Mohammad Hashem Sadraey
Southern New Hampshire University
Manchester, USA
Email: m.sadraey@snhu.edu

***Abstract*— The launch of fixed-wing Unmanned Aerial Vehicles has always been a challenging operation and witnessed various failures in the past decades. The current traditional ramp launchers are employing a rail and are powered by pneumatic/hydraulic systems. This paper discusses a new launch system for fixed-wing UAVs powered by linear synchronous motors and a special track. This novel idea has the potential to be developed to a new technique for launching fixed-wing UAVs. In this paper, linear synchronous motor is recommended as a source of generating launch thrust. The control of launch process is conducted utilizing an optimal controller. Advantages for this method are lower cost, higher reliability, stability, and safety. The verification and validation of the technique are documented using MATLAB simulation. This novel automatic launch system - powered by linear synchronous motors - provides a lower cost and a higher reliability than current launchers.**

Keywords- optimal control; unmanned aerial vehicles; launcher.

I. INTRODUCTION

The vast majority of fixed-wing Unmanned Aerial Vehicles (UAV) employ conventional launch and recovery techniques (i.e., conventional takeoff and landing). UAVs without a landing gear do not require a runway and are launched via various techniques, such as rail launchers; rocket launch; hand launch; and vertical takeoff.

A rail/ramp launcher eliminates the need for conventional landing gear for the purposes of takeoff. A ramp launcher is a mechanical device to accelerate a fixed-wing UAV to a minimum controllable airspeed before releasing it from launcher. The current traditional ramp launchers are employing a rail and are powered by pneumatic/hydraulic systems.

The current launch techniques have a few challenges including reliability, cost, stability, and safety. The electric launch technique that has not been employed so far in any unmanned aerial systems, have the potential to solve all these challenges. The novel technique presented in this paper is for the first time for launching an unmanned aircraft.

The pneumatic launching systems are typically designed as a catapult rail launcher. The energy storage is a compressed gas, usually the air is used, due to its availability and no cost. Air is pressurized by a compressor; and is stored in a high-pressure accumulator tank. The launch is performed by applying the compressed air force on UAV through a cylinder/pipe/tube along the ramp. The applied force can be regulated by adjusting the air pressure in order to support UAVs of different mass.

The hydraulic launching systems are much like the pneumatic ones. To perform a launch, a valve is quickly opened, so that the oil is pumped inside the cylinder to push the piston. Consequently, the gas is compressed on the other side.

The electric launching system is very much different from pneumatic and hydraulic ones. External power is usually used for starting the engine or maintenance activities on the UAV. The external power system allows operation of various electrical systems without discharging the onboard battery. The idea here is to use a special type of electric motors, referred to as the Linear Synchronous Motor (LSM). A LSM is a motor by which the mechanical motion is in synchronism with the magnetic field. A linear electric motor is a motor that has its stator and rotor unrolled. So, instead of producing a torque, it generates a linear force along its length.

To achieve benefits similar to those seen in hybrid-/all-electric ground-based and marine vehicles, large electric machines have been developed for aircraft electric propulsion [1][2]. Subsonic LSMs with high-temperature superconducting magnets are designed [3] to accelerate to a velocity of 1200 km/h in the near-vacuum tubes of 0.001 atm. A method for designing DC-excited **l**inear **s**ynchronous motor as a drive system is presented by [4]. Design and characteristic analysis on the short-stator LSM for high-speed maglev propulsion is provided by [5].

The application of LSMs has revolutionized the high-speed passenger transport systems and trains [6][7] in a number of countries including Europe, Japan, and China. Linear synchronous electric motors have been widely employed in industry applications such as in roller coasters. They can drive a linear motion load without gears and mechanical intermediates. For instance, the Incredible Hulk roller coaster [8] was designed in 1999 as part of a 1-billion-dollar park construction. In this roller coaster, 230 electric motors power a series of drive tires which provides 0 to 40 mph in 2 seconds at a 30° incline. Section III provides fundamentals and technical specification of LSMs.

In the past decade, a number of new launch techniques and new launch power sources have been developed. DARPA and Aurora have developed a new runway independent UAV launch and recovery system; called SideArm [9]; which is capable of both land and sea-based operations. It brings

 ISBN: 978-1-61208-966-9

runway independence to a new class of fixed wing UAVs. The SideArm is a self-contained, portable apparatus to launch and retrieve other unmanned aircraft from trucks, ships and fixed bases.

The Insitu [10] trailer-mounted Mark 4 launcher - a self-powered by an onboard diesel fuel generator and air compressor - is compatible with all of Insitu's unmanned aircraft. The setup of this launcher with a weight of 4,200 lb, a deployed length of 22 ft, and with two operators, takes about minutes. The AAI RQ-7 Shadow is also launched from a trailer-mounted pneumatic catapult. Its pneumatic launcher can accelerate the 170 kg air vehicle to 70 knots in 12 m.

The rest of the paper is organized as follow. In Section II, fundamentals of launch technique and governing equations will be described. The launch power system using Linear Synchronous Motors are discussed in Section III. The launch control system employing an optimal controller is presented in Sections IV and V. The verification and validation of the technique are documented using MATLAB simulation in Section VI.

II. FUNDAMENTALS OF RAIL LAUNCHERS

In a rail launch, the aerial vehicle is placed on the rail; when started, moves in the launcher along the rail for a very short time. In an ideal situation, a straight motion is desired for the UAV along the launcher. Major elements of a launcher (Figure 1) are ramp/slipway, elevation platform/mechanism, mobility wheels, transportation truck, power source, and push mechanism. Unlike missiles, there is often no rush in launching a UAV; thus, the azimuth and elevation platforms are adjusted by human operators, rather than through a closed-loop control system.

In the design of a launcher, parameters such as launcher length, launcher weight, launch angle, and the required force and power must be determined. Moreover, the type of source of launcher power (here, electric) needs to be formulated.

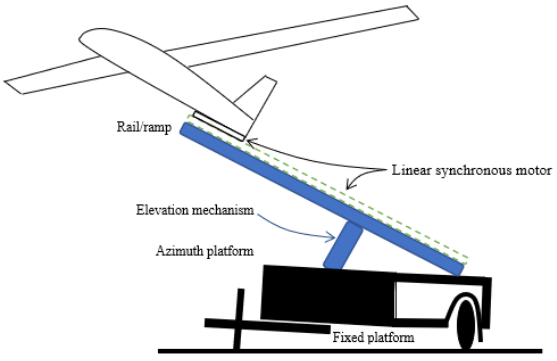

Figure 1. Major elements of a launcher

The launch process is basically a linear accelerated motion, where the UAV is accelerating along the ramp. The relationship between acceleration, launch speed, and launcher length has significant implications for launcher design. In launch operation, a large structural load on the UAV is often imposed, due to a high linear acceleration. When a moving object with an initial velocity of V_1 accelerates to a new velocity of V_2, the distance (x) covered is governed by the following equation:

$$V_L^2 - V_1^2 = 2aL_R \quad (1)$$

where "a" represents the linear acceleration. For an UAV launcher, the initial velocity is often zero, and the distance traveled is equal to the length of ramp launcher (L_R). In order for a launcher to create such acceleration, it must provide a sufficient launch force (F_L). Along the launcher ramp, sum of the forces along x-axis creates the acceleration. The contributing forces in this accelerated launching motion are launch force (including UAV engine thrust); F_L; UAV-ramp nonlinear friction force; F_f; UAV weight (W = mg), UAV drag (D), UAV lift (L), where m denotes the UAV mass. In the x direction (along the ramp), the momentum equation is:

$$F_L - F_f - D = ma \quad (2)$$

The aerodynamic forces of lift and drag [11] are:

$$L = \frac{1}{2}\rho V^2 S C_L \quad (3)$$

$$D = \frac{1}{2}\rho V^2 S C_D \quad (4)$$

where ρ is air density V is velocity, S is wing planform area, and C_L and C_D are the lift and drag coefficients respectively. The friction force is proportional to the UAV normal force (x-component of the weight minus lift), N. It is the product of the coefficient of friction μ with the normal force N, and acts to oppose the motion. Hence, the UAV-Ramp friction force (F_f) is:

$$F_f = \mu N \quad (5)$$

where μ is the friction coefficient between launcher rails and the UAV (indeed, two metals), and N denotes the normal force on the ramp. UAV weight and UAV lift are two contributing forces to the normal force. The ramp (Figure 2) has frequently a launch (i.e., climb) angle, θ.

$$N = W\cos\theta - L \quad (6)$$

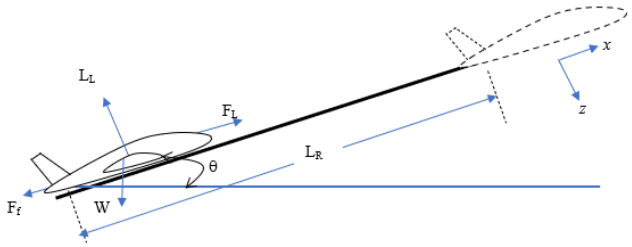

Figure 2. Contributing forces on a launcher

The friction coefficient (μ) between a UAV and the launcher rails is typically about 0.05-0.12. When the friction force from equations 5 and 6 is substituted into equation 4, we obtain:

$$F_L = W\cos\theta(1 + \mu) + ma \quad (7)$$

This is the force (F_L) that the launcher (indeed, the LSM) and UAV engine must provide to generate the desired acceleration during the launch operation. The engine thrust is contributing to the launch process; it will create a portion of the required launch force.

 ISBN: 978-1-61208-966-9

III. LINEAR SYNCHRONOUS MOTOR PROPULSION SYSTEM

A launcher requires a power supply for the activation of mechanisms such as the elevation platform. This paper introduces a new launch system for fixed-wing UAVs powered by LSM and a special track. Basically, the idea is that by launching the UAV along the rails at an angle, using LSMs and an electric power supply.

In general, a linear synchronous motor propulsion system is composed of two components, one is the LSM and the other is the power supply. A linear synchronous motor [12] is a motor by which the mechanical motion is in synchronism with the magnetic field. The force is generated as an action of traveling magnetic field produced by a poly-phase winding and an array of magnetic poles or a variable reluctance ferromagnetic rail. To reduce cost, synchronous linear motors rarely use commutators, so the rotor often contains permanent magnets, or soft iron.

To minimize the vehicle's weight, the electric system interconnections should be optimized (e.g., use smaller diameter wires). In wiring modules, it is recommended to place the wiring to one side of the module rack, so that, the other side will be free and available for temporary hookups. LSMs are currently in use in amusement parks around the world as a method to launch roller coasters, and they have been proven to be reliable at quickly and smoothly accelerating large payloads hundreds of times a day.

A linear electric motor is a motor that has its stator and rotor unrolled (one part over the launcher aril, and one part attached under the UAV). So, instead of producing a torque, it generates a linear force along its length. In a linear synchronous motor, the mechanical motion is in synchronism with the magnetic field. LSM drives a load (here, a UAV) linearly without a need to gears and mechanical intermediates. Linear synchronous motors are the low-acceleration, high speed and high-power motors with an active winding on one side of the air-gap and an array of alternate-pole magnets on the other side. Figure 3 illustrates the free-body diagram of a synchronous linear motor.

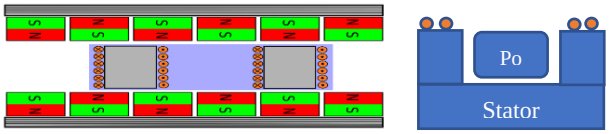

Top-view Front-view

Figure 3. Free-body diagram of a linear synchronous motor

The UAV is lay attached to a cart on the rails and will accelerate to the desired speed. The track (rail) contains on-board exciting magnets for LSM. Flux from the exciting magnet interacts with the traveling magnetic wave from the stator to generate launch force. The launch force is generated as an action of traveling magnetic field produced by a poly-phase winding and an array of magnetic poles or a variable reluctance ferromagnetic rail. The part that generates the magnetic flux or variable reluctance is referred to as salient pole rail. The part that generates the traveling magnetic field is referred to as the armature.

The length of required track is mainly a function of UAV weight, launch angle and launch power. LSMs benefit from high efficiency due to low magnetizing current and zero slip. This leads to a significant reduction of inverter rating, resulting in a substantial cost saving.

The LSM is selected as a source of generating launch thrust along the track. The model modeling of LSMs nonlinear, long, and complicated. The electromagnetic launch force developed by a LSM is obtained by:

$$F = \frac{P_{elm}}{u_s} \quad (8)$$

where P_{elm} is the electromagnetic power and u_s is the synchronous speed. The P_{elm} and u_s are functions of frequency of primary supply, the number of armature phase, rms value of the input voltage, and the rms value of armature current. The electromagnetic power and the synchronous speed are obtained by:

$$P_{elm} = mV_1 I_a cos(\phi) - mR_1 I_a^2 \quad (9)$$

$$u_s = 2f\tau \quad (10)$$

where m represents the number of armature phase number, $\cos(\phi)$ is the input power factor, I_a is the rms value of armature current, R_1 is armature winding resistance, and V_1 is the rms value of the input voltage, f is the frequency of primary supply, and τ is the mover (pole) pitch. The armature current is a function of desired launch force (F_L):

$$I_a = \frac{F_L u_s \left(\frac{1}{\eta} - 1\right)}{\rho_w l_w j_c} \quad (11)$$

where j_c is the amplitude of linear current density, ρ_w is the electrical resistivity of the primary windings, and l_w is the primary windings length. The parameter η is estimated in 0 - 1 range and will be finalized during the design. The two most generally used conductors (for wire windings) are copper and aluminum. Copper has a higher conductivity (about 40% more); is more ductile; has relatively high tensile strength; and can be easily soldered. Copper is more expensive and heavier than aluminum.

This launch system has a number of significant advantages as compared with conventional launchers. Loading UAV and setting them up would also take much less time and effort than other power systems.

IV. OPTIMAL CONTROL

To optimize the launch operation, a closed-loop optimal control system is employed. The optimal control - Linear Quadratic Regulator (LQR) [13] - is based on the optimization of some specific performance criterion; or Performance Index; J. In this technique, no disturbance, noise, or uncertainty is considered.

We are interested in minimizing the error of the system; any deviation from equilibrium point is considered an error. To this end, an error-squared performance index is defined. For a system with one state variable, x_1, we have

$$J = \int_0^{t_f} [x_1(t)]^2 dt \quad (12)$$

 ISBN: 978-1-61208-966-9

An optimization technique for a dynamic system in state-space format is employed. The LQR is an optimal controller and is defined as follows. The system of interest is of the form:

$$\dot{x} = Ax + Bu \quad (13a)$$
$$y = Cx + Du \quad (13b)$$

Given the *weighting matrices* Q and R, the design task is to find the optimal control signal u(t) such that the quadratic cost function:

$$J = \frac{1}{2}\int_0^\infty (x^T Q x + u^T R u)dt \quad (14)$$

is minimized. The solution to this problem is:

$$u = -Kx \quad (15)$$

where

$$K = R^{-1}B^T P \quad (16)$$

and P is the unique, positive semi-definite solution to the Algebraic Riccati Equation (ARE):

$$PA + A^T P + Q - PBR^{-1}B^T P = 0 \quad (17)$$

Based on this technique, the LQR gains are calculated using a MATLAB code, and then a control system is designed. The engineering judgment skill must be utilized in the selection of Q and R. Tuning techniques are recommended in the determination of design parameters. For instance, Q and R must be such that the detectability (i.e., $(\sqrt{Q}, A)$ must be detectable) and observability requirements are met.

The LQR is a popular optimal control technique that has been successfully applied to control several UAV configurations. The LQR was successfully used [14] in stabilizing a Yamaha RMAX helicopter.

V. LAUNCH CONTROL SYSTEM

The electromechanical mathematical model of the stage with loads is formulated by employing the governing equation presented in Section III. The equation of motion can be stated in terms of electric current (i) and distance travelled (x) as:

$$m\ddot{x}(t) = F_e - F_f - D \quad (18)$$

By inserting models of electromagnetic force, friction force, and drag into equation 18, we obtain:

$$m\dot{V}(t) = K_e i(t) - K_f \dot{x}(t) - K_D \dot{x}(t) \quad (19)$$

or,

$$\dot{V}(t) = \frac{K_e}{m} i(t) - \frac{K_f + K_D}{m} \dot{x}(t) \quad (20)$$

where Fe denotes the electromagnetic force (here, the launch force, F_L), K_e represents thrust coefficient and the K_f and K_D denote friction and drag factors respectively. The inherent force ripple and the effects of the magnetic flux distortions and saturations are neglected for simplicity. The launch angle is assumed to be constant, and two parameters of velocity (V) and acceleration (a) are controlled. By reformatting equation 20, the state space representation of the launcher from is obtained:

$$\begin{bmatrix}\dot{x}\\ \dot{V}\end{bmatrix} = \begin{bmatrix}0 & 1\\ 0 & -\frac{K_f+K_D}{m}\end{bmatrix}\begin{bmatrix}x\\ V\end{bmatrix} + \begin{bmatrix}0\\ \frac{K_e}{m}\end{bmatrix} i \quad (21)$$

According to Equation (21), and the relation between linear acceleration and linear speed, the block diagram of the linear motor positioning system is illustrated in Figure 4.

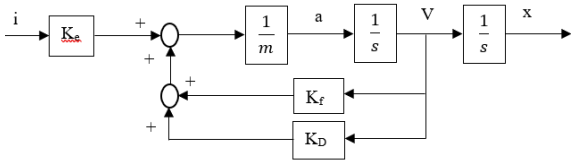

Figure 4. Block diagram of the electric launcher control system

In literature, various aspects of LSMs including their modeling, analysis, design, and control have been discussed. For instance, Ref. [5] has presented the design and characteristic analysis on the short-stator LSM for high-speed Maglev propulsion. Here, we use a linear model, since the objective of this paper is mainly to provide the effectiveness of hybrid launch system.

Two important motion parameters need to be controlled during a launch operation: 1. Velocity (V), 2. Acceleration (a). This objective requires a closed-loop feedback control system using an appropriate control law. The goal of control law is to have a near-constant acceleration at start of the launch but ease off slightly at the end. Proximity sensors should be installed at increments along the track to measure and report UAV position and speed to calculate the linear acceleration. For safety reasons, some other parameters such as the armature current (i) of LSMs may be controlled too.

The block diagram of closed-loop control system of the launch operation is shown in Figures 5. There are motion sensors for three outputs: 1. Position is measured, 2. Velocity is calculated by differentiation of position, and incorporating time of measurement, 3. Acceleration is calculated by differentiation of velocity, and incorporating time of measurement.

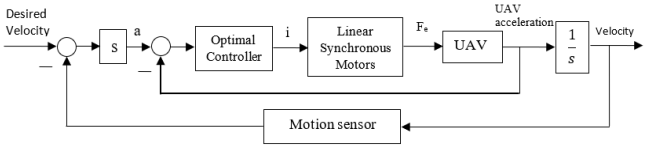

Figure 5. Block diagram of control system of the launch operation

The controller sends full-power signal to the motor when triggered. Due to the linear motion of the UAV along the track, an optimal control law will suffice in effectively controlling the launch operation. This dynamic system is modeled with two state variables, one input, and two outputs. The state space model is:

$$A = \begin{bmatrix}0 & 1\\ 0 & -\frac{K_f+K_D}{m}\end{bmatrix},\ B = \begin{bmatrix}0\\ \frac{K_e}{m}\end{bmatrix},\ C = \begin{bmatrix}1 & 0\\ 0 & 1\end{bmatrix},\ D = \begin{bmatrix}0\\ 0\end{bmatrix} \quad (22)$$

The state and output variables are:

$$x = \begin{bmatrix}x\\ V\end{bmatrix} \text{ and } y = \begin{bmatrix}x\\ V\end{bmatrix}$$

The control signal u is given (Figure 6) by

$$u = k_1(r - x_1) - k_2 x_2 = k_1 r - (k_1 x_1 + k_2 x_2) \quad (23)$$

For a zero-reference input (i.e., r = 0):

$$u = -k_1 x_1 - k_2 x_2 = -Kx \quad (24)$$

To determine the state-feedback gain matrix K, where

$$K = [k_1 \ k_2] \quad (25)$$

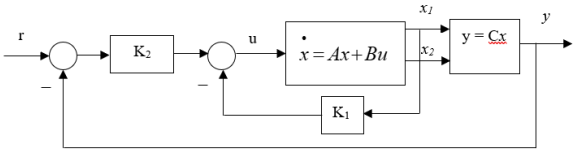

Figure 6. Quadratic optimal regulator system for the launcher

The modified state-space representation is developed by incorporating two feedbacks into the original plant:

$$\dot{x} = Ax + B(-Kx + k_1 r) = (A - BK)x + Bk_1 r \quad (26)$$

Therefore, the revised state-space model matrices are:

$$A1 = A - B*K;\ B1 = B*K(1);\ C1 = C;\ D1 = D \quad (27)$$

The new state-space model can be used in the simulation to determine the behavior of the system. Two objectives of control are: 1. Keep the acceleration below 7g, 2. Keep the launch speed to follow the desired velocity profile. UAV weight plays a major role in control parameters due to incline angle. The controller is generating a signal to the actuators (i.e., LSM) based on the control law. The LQR gains are functions of LSM features and UAV weight. Tabular values for LQR gains may be determined for various UAVs weights.

The main output of the LQR controller is the rms value of armature current (I_a or just i), which will be the input to the LSM. The main output of the LSM and the track is the launch force (F), which will be the input to the UAV. To reduce "jerk", we need to have an overdamped velocity profile. To have a successful launch, the wind speed and direction should be measured at the launch site and incorporated in the control process.

VI. Simulation and Results

In order to validate the design outcome, a launch system including a linear model of LSM for launching a UAV with a mass of 20 kg has been simulated by matlab Simulink. It is desired that the UAV reaches the velocity of 10 m/sec along the track before the end of launch operation.

The simulation is presented to demonstrate the efficacy of the proposed launch system with the control algorithm. Figures 7 through 11 illustrate the simulation results for: 1. LSMs current in Amps, 2. Velocity of UAV in m/sec, 3. Vehicle non-dimensionalized acceleration, 4. UAV displacement in meter, 5. Force generated by LSM in N, and 6. Electric power provided to LSMs in W, respectively. It is assumed that voltage for LSMs is 120 Volts.

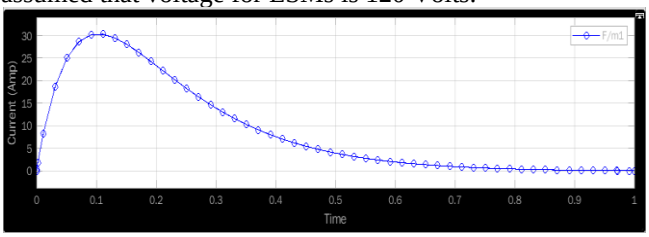

Figure 7. Variations of LSM current (in Amps)

From Figure 7, the maximum current is about 30 Amps at 0.1 seconds to the launch. When the UAV reaches the desired velocity, the LSM current is reduced to almost zero.

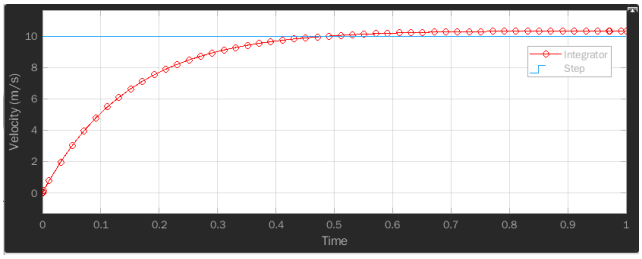

Figure 8. Variations of UAV velocity (in m/sec)

In Figure 8, the desired velocity of 10 m/sec (blue line) is a given value and shown. It can be seen that the UAV reaches this velocity in about 0.5 seconds (intersection of red graph with blue line) and continue to increase to about 10.5 m/sec due to the UAV linear momentum. Since no brake is considered in the launch system, the velocity is not reduced back to 10 m/sec during launch.

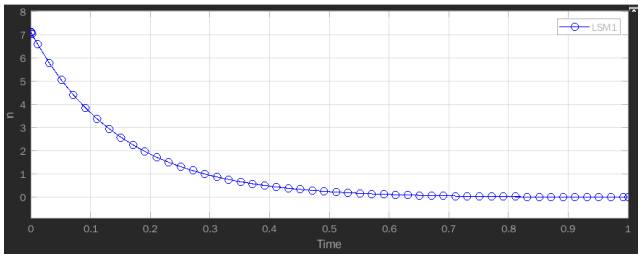

Figure 9. Variations of normalized acceleration

As shown in Figure 9, the maximum non-dimensionalized acceleration, i.e., (in g) is about 7, it happens in the beginning of launch. When the vehicle reaches the desired velocity, the acceleration will become zero.

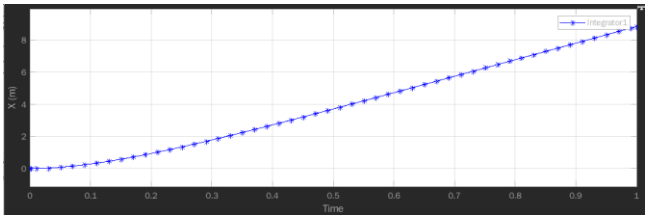

Figure 10. Variations of vehicle displacement (in m)

As shown in Figure 10, after 1 second, the vehicle has displaced about 9 m. From this part of the simulation, it is concluded that a launch track with the length of 9 meters is required to launch a UAV with a mass of 20 kg. To have a launch site for UAVs with various masses, a longer launch track should be constructed.

As Figure 11 indicates, the maximum force generated by LSM is 1400 N at the beginning of launch. When the vehicle reaches the desired velocity, this force will become almost zero. Afterward, a small amount of force is needed to cover the track friction and UAV drag.

 ISBN: 978-1-61208-966-9

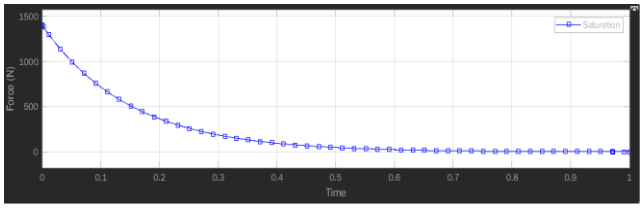

Figure 11. Variations of the LSM generated force

The maximum electric power provided to LSMs is 3.5 kW after about 0.1 seconds. The engine of the vehicle should be started when the vehicle reaches the desired velocity (i.e., before UAV reaches the end of launch track). However, if the UAV own engine is operating along the track (concurrent with LSM), the vehicle will have a much faster velocity at the end of the launch operation.

By examining the simulation results, one can conclude that launch operation utilizing electric power is feasible. Using the LQR controller, the UAV is tracking and following the desired velocity on the track. For other UAVs with different weights, the LQR gains should be adjusted/changed. As the simulation results indicate, the launch operations using LSM is successful. Since the vehicle is along the ramp and uses a special rail connection, the UAV is stable and reliable.

Moreover, this system can be employed over and over again for various UAVs, so the overall launch cost is much lower than a vertical launch. The investment for the track and LSM is for a long run application. Furthermore, there is no possibility of explosion by UAV engines, since the launch power system is of electric type.

VII. Conclusion and Future Work

This paper presented a new launch system for fixed-wing UAVs powered by linear synchronous motors and a special track. This novel idea has the potential to be developed to a new technique for launching fixed-wing UAVs. In this paper, LSM was recommended as the source of generating launch force. The control of launch process was conducted utilizing an optimal controller. The most notable advantages of this technique are lower cost, higher reliability, stability, and safety. A difficulty in this technique is a relatively heavy equipment. For the future work, the next technical step would be to focus on reducing weight of the power system and improving the efficiency of this electric launcher.

References

[1] Z. Xiaolong, B. Cheryl, T. O'Connell, and K. Haran, "Large electric machines for aircraft electric Propulsion", IET Hybrid Propulsion for Aviation, Vol. 12 Issue 6, 2018, pp 767-779.

[2] B. Sarlioglu and C. T. Morris, "More electric aircraft: review, challenges, and opportunities for commercial transport aircraft", IEEE Transactions *on* Transportation Electrification, 2015, 1, pp. 54–64

[3] J. F. Gieras, J. P. Zbigniew, and T. Bronislaw, "Linear synchronous motors: transportation and automation systems", CRC Press, 2018

[4] R. S. Fattahpour and A. Shiri, "A New Method for Designing DC-Excited Linear Synchronous Motor", 11th Power Electronics, Drive Systems, and Technologies Conference, 2020, IEEE Xplore, pp 1-6

[5] H. Cho, H. Sung, S. Sung, D. You, and S. Jang, "Design and Characteristic Analysis on the Short-Stator Linear Synchronous Motor for High-Speed Maglev Propulsion", IEEE Transactions on Magnetics, Vol. 44, No. 11, pp. 4369-4372, Nov 2008

[6] H. Ohsaki, "Linear Drive Systems for Urban Transportation in Japan, Proceedings of the Maglev Conference", Yamanashi, Japan, April 1998, pp. 29

[7] M. Mossi and P. S. Rossel, "A revolution in the high-speed passenger transport systems", In Proceedings of the 1st Transport Research Conference, pp 1–16, Ascona, Switzerland, 1–3 March 2001

[8] A. Stilwell, "19 For 99: Incredible Hulk Coaster at Universal's Islands", July 4, 2019

[9] M. D. Adamski, R. Root Jr., and A. M. Watts, "UAV recovery system", US Patent US7219856 B2, 2007

[10] Scan Eagle fact sheet and specification, Insitu.com, Insitu, A Boeing company, 2020

[11] M. H. Sadraey, "Aircraft Performance Analysis: An Engineering Approach", CRC Press, 2017

[12] R. J. Kaye and E. Masada, "Comparison of Linear Synchronous and Induction Motors", Urban Maglev Technology Development Program, Sandia National Laboratories, FTA-DC-26-7002.2004.01, June 2004

[13] B. D. O. Anderson and J. B. Moore; "Optimal Control - Linear Quadratic Methods"; Dover, 2007

[14] F. Kendoul, "Survey of advances in guidance, navigation, and control of unmanned rotorcraft systems", Journal of Field Robotics, vol. 29, no. 2, 2012, pp 315-378

 ISBN: 978-1-61208-966-9